

Stability properties of the two-component Bose-Einstein condensate

Patrik Öhberg

Department of Physics, Royal Institute of Technology Lindstedtsvägen 24, S-10044 Stockholm, Sweden

(Received 14 May 1998; revised manuscript received 10 August 1998)

The two-component Bose-Einstein condensate is known to break its symmetry spontaneously. The stability of the symmetric solution has been investigated by solving the ground-state density profiles for different parameter regimes. We emphasize the importance of the trap geometry for the formation of the condensate. [S1050-2947(99)00201-2]

PACS number(s): 03.75.Fi, 05.30.Jp

I. INTRODUCTION

After the realization of the atomic Bose-Einstein condensation [1–3] it was found that the $|F=2, m=2\rangle$ and $|F=1, m=-1\rangle$ substates of Rb can form overlapping condensates in a magneto-optical trap with the two species slightly offset relative to one another by gravity [4]. Recent progress has been made in trapping two species with the same magnetic moment, $|F=2, m=1\rangle$ and $|F=1, m=-1\rangle$, and they are therefore sharing the same trap center and not separated by gravity [5].

In this paper we investigate the spontaneous breaking of the cylindrical symmetry which these two-component condensates can undergo when trapped in identical external potentials. This effect, where the condensates go from a centered geometry to two separated condensates, has been investigated numerically in earlier works [6–11], mainly concentrating on elementary excitations [12–14], since these are very sensitive to the actual geometric configuration of the condensates. In this paper we calculate the condensate densities and ground-state energies at zero temperature using well-known Gross-Pitaevskii equations generalized to the two-component situation. The main results are calculations for density distributions at different interaction strengths between the two species. We find a nontrivial dependence on the trap geometry, where the aspect ratio (Ω_r/Ω_z) plays a crucial role when determining the stable configurations. It is generally accepted that the double condensate can separate in traps of modest aspect ratios as in the present laboratory two-component traps, where the aspect ratio has been $\Omega_r/\Omega_z=1/\sqrt{8}$. Our calculations show that this may not always be the case for the large aspect ratio traps recently utilized for single condensates using optical trapping [15].

The organization of the present paper is as follows. Section II presents the coupled Gross-Pitaevskii equations for the double condensate. In Sec. III we justify the presence of a symmetry breaking by doing a simple variational calculation for the spherically symmetric trap. The results of the numerical calculations are presented in Sec. IV. The main results and conclusions are presented in Sec. V.

II. BASIC EQUATIONS

We consider a two-component Bose condensed gas in the external harmonic potentials

$$V_i(r, z) = \frac{1}{2}m(\Omega_r^2 r^2 + \Omega_z^2 z^2), \quad i = 1, 2, \quad (1)$$

with the trap frequencies Ω , and assume a pair potential of the atom-atom interaction of the form $V_i = v_i \delta(\mathbf{r} - \mathbf{r}')$ with

$$v_i = \frac{4\pi\hbar^2 a_i}{m}, \quad i = 1, 2, 3, \quad (2)$$

where a_1 and a_2 stand for the intraspecies scattering lengths, a_3 is the scattering length between the two different atoms, and m is the mass of the atoms which is taken to be the same for both species. The mean-field theory at zero temperature provides a good description of a dilute Bose-Einstein condensed gas. In particular, the dynamics of a two-component condensate can be described by the generalized Gross-Pitaevskii equations

$$i\hbar \frac{\partial}{\partial t} \Psi_1(\mathbf{r}) = \left[-\frac{\hbar^2}{2m} \nabla^2 + V_1(r, z) + v_1 |\Psi_1(\mathbf{r})|^2 + v_3 |\Psi_2(\mathbf{r})|^2 \right] \Psi_1(\mathbf{r}), \quad (3a)$$

$$i\hbar \frac{\partial}{\partial t} \Psi_2(\mathbf{r}) = \left[-\frac{\hbar^2}{2m} \nabla^2 + V_2(r, z) + v_2 |\Psi_2(\mathbf{r})|^2 + v_3 |\Psi_1(\mathbf{r})|^2 \right] \Psi_2(\mathbf{r}), \quad (3b)$$

where Ψ_i are the macroscopic wave functions of the condensates and the normalization chosen such that

$$\int d\mathbf{r} |\Psi_i(\mathbf{r})|^2 = N_i \quad i = 1, 2. \quad (4)$$

Assuming a time dependence of the form

$$\Psi_i(\mathbf{r}) = \Psi_i^g(\mathbf{r}) e^{-i\mu_i t/\hbar}, \quad (5)$$

with $\{\Psi_1^g, \Psi_2^g\}$ chosen real, we obtain the Gross-Pitaevskii ground-state equations from Eqs. (3a) and (3b):

$$\mu_1 \Psi_1^g(\mathbf{r}) = \left[-\frac{\hbar^2}{2m} \nabla^2 + V_1(r, z) + v_1 \Psi_1^g(\mathbf{r})^2 + v_3 \Psi_2^g(\mathbf{r})^2 \right] \Psi_1^g(\mathbf{r}), \quad (6a)$$

$$\mu_2 \Psi_2^g(\mathbf{r}) = \left[-\frac{\hbar^2}{2m} \nabla^2 + V_2(r, z) + v_2 \Psi_2^g(\mathbf{r})^2 + v_3 \Psi_1^g(\mathbf{r})^2 \right] \Psi_2^g(\mathbf{r}). \quad (6b)$$

III. STABILITY OF THE GROUND-STATE SOLUTIONS

The two-component ground-state solutions of the Gross-Pitaevskii equations are surprisingly rich in their nature. It is known from earlier investigations [6,11] that the two-component condensate can undergo a symmetry breaking from a symmetric situation where the two condensates sit right on top of each other with the possibility of one of the condensates forming a shell around the other one, to an asymmetric formation where the condensates are displaced with respect to each other. This symmetry breaking can happen if the particle number or the interaction strength v_3 is sufficiently large. It is easy to show that a symmetry breaking may occur, by using a naive variational calculation where we obtain the ground-state energy E from the energy functional

$$E[\Psi_1^g, \Psi_2^g] = \int d\mathbf{r} \left(\sum_{i=1}^2 \left\{ \frac{\hbar^2}{2m} |\nabla \Psi_i^g|^2 + V_i(r, z) |\Psi_i^g|^2 + \frac{1}{2} v_i |\Psi_i^g|^4 \right\} + v_3 |\Psi_1^g|^2 |\Psi_2^g|^2 \right) \quad (7)$$

using the Gaussian trial functions

$$\Psi_i^g(r, z) = \sqrt{N_i} \pi^{-3/4} e^{-(1/2)[r^2 + (z - z_i)^2]}, \quad i = 1, 2 \quad (8)$$

where we for simplicity have assumed isotropic symmetry with the scaling factor $\sqrt{\hbar/m\Omega}$ in the r and z directions. The ground-state energy will then be a function of the displacements z_1 and z_2 ,

$$E = 3N_1 + 3N_2 + N_1 z_1^2 + N_2 z_2^2 + \frac{v_1 N_1^2 + v_2 N_2^2}{2(2\pi)^{3/2}} + \frac{N_1 N_2 v_3}{(2\pi)^{3/2}} e^{-(1/2)(z_1 - z_2)^2}. \quad (9)$$

Setting the derivatives $\partial E / \partial z_i$ equal to zero gives the equations

$$z_1 = \frac{v_3 N_2}{2(2\pi)^{3/2}} (z_1 - z_2) e^{-(1/2)(z_1 - z_2)^2}, \quad (10)$$

$$z_2 = \frac{v_3 N_1}{2(2\pi)^{3/2}} (z_2 - z_1) e^{-(1/2)(z_1 - z_2)^2}. \quad (11)$$

Here we already see that one solution is $z_1 = z_2 = 0$. If we further assume $N_1 = N_2 = N$ and $v_1 = v_2$, the system is fully symmetric ($z_1 = -z_2$), and we can express z_1 and z_2 with the variable $z_0 = z_1 - z_2$. Equations (10) and (11) can then be combined, giving the solution

$$z_0 = \sqrt{2 \ln \left(\frac{v_3 N}{(2\pi)^{3/2}} \right)}. \quad (12)$$

In order to obtain the global minimum of the energies, we insert solution (12) into Eq. (9) and compare the result with the zero solutions. If the condition

$$\frac{v_3 N}{(2\pi)^{3/2}} > 1 \quad (13)$$

is fulfilled, the condensates are separated, otherwise they sit on top of each other.

This crude variational calculation does not take into account the fact that the condensates can form shell structures, and consequently predicts the onset of symmetry breaking too early as a function of $v_3 N$. In Sec. IV we investigate the extent of the stable symmetric situation, depending on different trap geometries. We also look at the stability of the symmetric shapes once we are in the region where an asymmetric situation is favored.

IV. NUMERICAL METHODS AND RESULTS

When solving the Gross-Pitaevskii equations in a cylindrical symmetry, it is most favorable to discretize the solutions and the derivatives. In cylindrical coordinates the condensate densities or wave functions are expressed as matrices where rows and columns correspond to the radial and the z coordinate. The time-independent Gross-Pitaevskii equation (6) is then solved with the method of steepest descent, which has been successfully used in earlier works on the nonlinear Schrödinger equation [16,17]. This is simply solving the time-dependent Gross-Pitaevskii equation with an imaginary time which turns the problem into solving a diffusion equation. The true time-dependent problem is, of course, solved in the same manner where the solution has to be split into real and imaginary parts, in contrast to the time-independent case where one can assume the solution to be real. It is important to note that the wave functions have to be normalized after each iteration due to the nonlinear terms. The numerical method used for solving the time-dependent Gross-Pitaevskii equation has often been a second-order implicit finite-differencing scheme (for a nice example using this approach, see Ref. [18]). The method used here is also a method of finite differencing, where the time step is split into two parts [19], giving an explicit second-order differencing scheme. It is, in fact, also possible to use a single time step, but this scheme is only stable for short times, and requires at least a factor of ten smaller time steps.

In the results presented here we have scaled the r and z coordinates with $\sqrt{\hbar/m\Omega_r}$, where the mass m along with the trap frequencies were chosen to be the same for both species. All energies were correspondingly expressed in units of $\hbar\Omega_r/2$, and the time in units of $2/\Omega_r$. Throughout these calculations (except for Fig. 5) we have used $N = N_1 = N_2 = 2100$, with $v_1 = 0.045$ and $v_2 = 0.02$, which corresponds for v_1 in the case of rubidium atoms ($a = 109a_0$) to a trap frequency of $\Omega_r = 2\pi \times 10$ Hz. The interaction strengths v_1 and v_2 were chosen not to be the same in order to show the effects of the interactions more transparently. In the experiments with rubidium, the ratio of v_1 to v_2 is approximately 1.062 [20].

When solving the Gross-Pitaevskii equation with the steepest-descent method, it is not obvious that it will give a

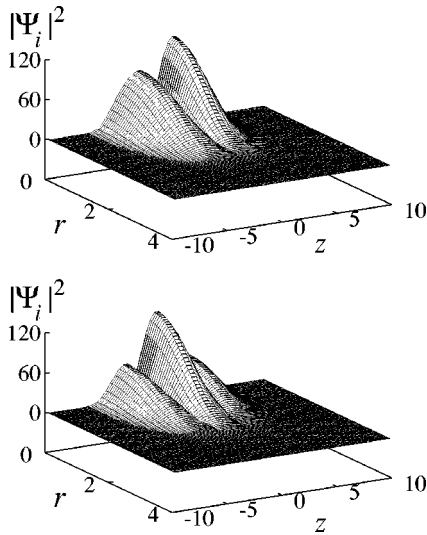


FIG. 1. Two possible stable formations of the condensates in a cigar-shaped trap with $\Omega_r/\Omega_z = \sqrt{8}$ and $v_3 = 0.05$. At the top we see the ground state with $E = 7.618$ ($\mu_1 = 5.068$ and $\mu_2 = 4.258$). The two condensates are clearly separated. At the bottom is the symmetric shell formation with $E = 7.666$ ($\mu_1 = 5.134$ and $\mu_2 = 4.268$). All energies are scaled by $\hbar\Omega_r/2$.

solution corresponding to the ground state, since the solution might converge only to a local minimum. Such a local minimum, achieved with a sufficiently large interaction strength between the condensates, may be the shell formation, whereas the displaced formation may correspond to a state with lower energy. This is shown in Figs. 1 and 2 for two different trap geometries with $\Omega_r/\Omega_z = \sqrt{8}$ and $\Omega_r/\Omega_z = 27$; the latter is the aspect ratio of the atomic clouds in optical traps recently presented for single condensates. In Fig. 1, the ground state, calculated using Eq. (7), is the symmetry-broken case with energy $E/N = 7.618$, as compared with the energy $E/N = 7.666$ of the symmetric case. At

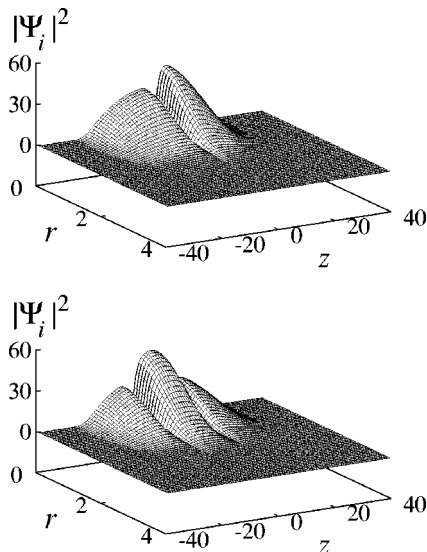


FIG. 2. The same situation as in Fig. 1 with $\Omega_r/\Omega_z = 27$ and $v_3 = 0.1$. The energies here are $E = 4.903$ ($\mu_1 = 2.798$ and $\mu_2 = 2.552$) for the symmetry-broken case and for the symmetric ground state $E = 4.900$ ($\mu_1 = 2.791$ and $\mu_2 = 2.533$).

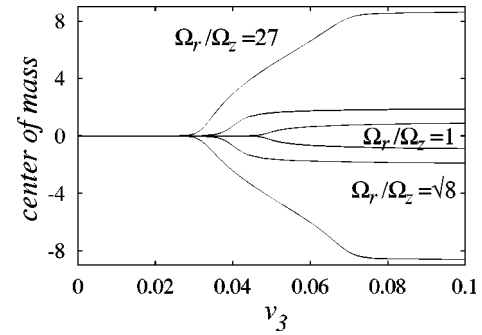


FIG. 3. The center of mass in the z direction, shown at three different trap geometries $\Omega_r/\Omega_z = 1$, $\Omega_r/\Omega_z = \sqrt{8}$, and $\Omega_r/\Omega_z = 27$. The more cigar shaped they are, the more separated the condensates become. The center of mass is calculated for the symmetry-broken configurations whenever the interaction strength allows it. For $\Omega_r/\Omega_z = 27$ the symmetric configuration may be the ground state, resulting in a center of mass at $z = 0$. The different interaction strengths $v_1 = 0.045$ and $v_2 = 0.02$ have no visible effect on the distance between the condensates.

this repulsion strength, $v_3 = 0.05$, the condensates gain energy by separating. In Fig. 2, on the other hand, the symmetry-broken configuration has the energy $E/N = 4.903$ as compared with the value 4.900 for the symmetric case, which thus is the ground state. Here the repulsion is even stronger, $v_3 = 0.1$, and hence the large aspect ratio is found to allow a symmetric ground state even for a strong repulsion. The explanation seems to be that the cigar-shaped trap allows one to push one condensate far enough away from the center to minimize the energy more efficiently than by displacing the condensates asymmetrically. The energy difference between the two stable solutions is small; their relative stability, however, is good (see below).

In the numerical calculations, the symmetric or symmetry-broken configurations have been found by making an ansatz of two Gaussians sitting on top of each other or separated, respectively. For small interaction strengths v_3 , the difference between the two cases is indiscernible, and we found the condensate displacements to emerge gradually when the repulsion v_3 is increased. This emerging displacement is shown in Fig. 3 for three aspect ratios $\Omega_r/\Omega_z = 1$, $\sqrt{8}$, and 27. We find that the separation appears for lower interaction strengths the larger the aspect ratio is. However, the result of Fig. 2 shows that, for the high aspect ratio $\Omega_r/\Omega_z = 27$, the symmetric solution has a lower energy. This can be verified by using the symmetric ansatz as the starting point for the calculation.

In Fig. 4 we show the difference between the ground-state energies for different trap geometries. Here we can see that for sufficiently large aspect ratios ($\Omega_r/\Omega_z > 22$) and a strong interaction, $v_3 = 0.1$, the ground state may be the symmetric formation. For $v_3 = 0.05$ the symmetry is broken for even lower aspect ratios ($\Omega_r/\Omega_z = 9$). The results in Fig. 4 rely on the fact that the different configurations are stable. If the interaction strength v_3 is decreased even further, the solution will always converge toward the symmetric configuration (see Fig. 3), indicating that the symmetry-broken solution has become unstable. The aspect ratio played a crucial role in the results shown in Figs. 1 and 2, where the high-aspect-ratio trap gave a symmetric ground state. A high aspect ratio,

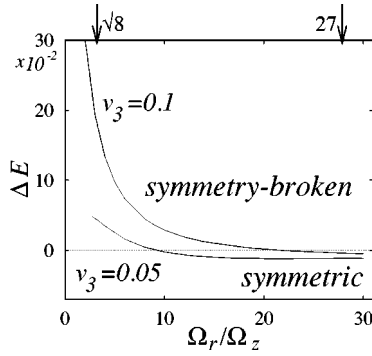


FIG. 4. The difference between the ground-state energies for the symmetric and symmetry-broken formations, $\Delta E = (E_{\text{symmetric}} - E_{\text{symmetry-broken}})/N$, show that the symmetric case may possess the lowest energy even if the interaction strength is large, provided that the aspect ratio of the trap is high enough.

however, is no guarantee of symmetric ground states. To illustrate this, in Fig. 5 we show the ground-state energy as a function of v_1 for the symmetric and symmetry-broken configurations, where the aspect ratio ($\Omega_r/\Omega_z=27$) and v_2 ($v_2=0.02$) are kept constant. Here we see that for $0.002 < v_1 < 0.043$ the symmetry is broken. The point where $v_1=v_2$ deserves special attention. One possible symmetric solution then consists of two identical condensates sitting on top of each other. The corresponding energy is then in fact much higher, $E/N=5.235$, than for the symmetric shell structures. This is clearly an unstable configuration, which can also be seen if the symmetric solution is perturbed simply by giving it a weak random kick, resulting in a convergence toward the symmetry-broken configuration.

Now one might ask how stable the shell formations shown in Figs. 1 and 2 are, if we are in a parameter region where the symmetry-broken situation is the ground state. In order to obtain some feeling for the stability of these systems, we take the symmetric solutions from Figs. 1 and 2, and solve the time-dependent Gross-Pitaevskii equations, where we have inserted a linear potential which pulls the two condensates in different directions:

$$V_i^p(z, t) = \frac{1}{2} k_i \left[1 - \cos\left(\frac{\pi}{t_{\text{max}}} t\right) \right] z, \quad i = 1, 2. \quad (14)$$

Here k_i is chosen such that, at the time $t=t_{\text{max}}$, the effective potentials $V_i^{\text{eff}}(r, z) = V_i(r, z) + V_i^p(z, t)$ have their minima at $z_i = B_i k_i / 2$, where B_i is the scaling factor:

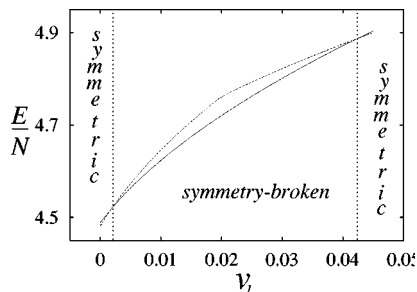


FIG. 5. By varying the interaction strength v_1 with $v_2=0.02$, $v_3=0.1$, $N=2100$, and $\Omega_r/\Omega_z=27$, it is possible to obtain a lower energy with the symmetry-broken configuration (solid line) for $0.002 < v_1 < 0.043$.

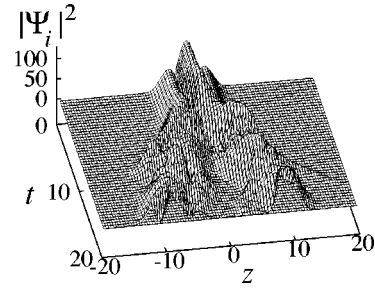


FIG. 6. The condensates are pushed in opposite z directions starting from the symmetrical situation. The symmetry is fully broken at $t=8$. The trap geometry here is $\Omega_r/\Omega_z=\sqrt{8}$ with $v_3=0.05$. The density is plotted at $r=0$. The time is in units of $2/\Omega_r$, and the spatial coordinates in units of $\sqrt{\hbar/m\Omega_r}$.

$$B_i = \left(\frac{\Omega_{r_i}}{\Omega_{z_i}} \right)^2. \quad (15)$$

In Fig. 6 we show the time evolution of the condensates with $\Omega_r/\Omega_z=\sqrt{8}$, when the potential minima at $t=t_{\text{max}}=20$ are at $z=\pm 8$. Here the symmetric configuration is expected to be locally stable only. The condensates can already be seen to start separating at $t=8$. Because of the rapid symmetry breaking, we also see “sloshing” effects when the condensates start to oscillate in the new effective potentials. In Fig. 7 we present the same calculation for the high-aspect-ratio situation, with $\Omega_r/\Omega_z=27$ at a relatively strong interaction strength $v_3=0.1$. The condensates remain in a shell formation, and show no tendency toward symmetry breaking. Decreasing the interaction strength to $v_3=0.03$ drastically changes the picture, as seen in Fig 8. The symmetry is now completely broken around $t=20$, where the condensates slide over in different directions to form the two separated peaks. With this interaction, we have moved into the regime where the interaction v_3 is not strong enough to prevent the symmetry breaking.

The time-dependent calculations serve as an illustration of how stable the symmetric configurations are. The separation of the minima of the effective potentials is a measure of the force acting on the condensates, pulling them apart. In order to draw any conclusions from the point where the symmetry is broken, the force pulling the condensates apart must be applied adiabatically. In other words, sloshing effects due to a too abruptly applied force should be avoided.

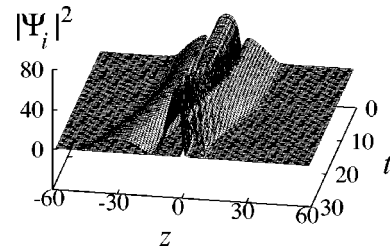


FIG. 7. The same situation as in Fig. 2 with $\Omega_r/\Omega_z=27$ and $v_3=0.1$. The more pronounced cigar shape makes the symmetric situation more stable. The condensates remain centered, and only slightly change their shapes. For $t > 20$ the effective potentials from Eq. (14) are kept constant with their minima at $z = \pm 30$.

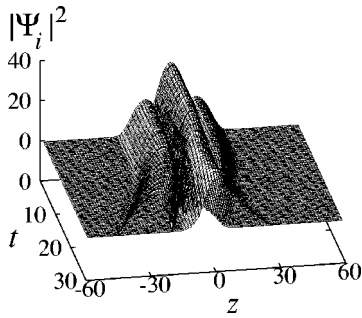


FIG. 8. Decreasing the interaction strength to $v_3=0.03$ with $\Omega_r/\Omega_z=27$ dramatically changes the stability of the symmetric formation as compared to Fig. 7.

V. CONCLUSIONS

The two-component Bose-Einstein condensate shows surprisingly complex behavior compared to the single condensate. The symmetry breaking discussed is a typical feature of the two-component condensate. In this paper we have investigated the different geometric configurations the condensates can take, as well as their stability. This has been done by solving both the stationary and time-dependent Gross-Pitaevskii equations, which enabled us to investigate the stability of the different formations when disturbed by an external time-dependent force. The main results show that the trap geometry, or the aspect ratio, plays an important role when determining the stable configurations. The calculations show that, with modest aspect ratios ($\Omega_r/\Omega_z \sim \sqrt{8}$), the expected symmetry breaking is favored at increasing interaction

strengths or particle numbers. The symmetry breaking can, however, be suppressed if the external potentials are squeezed to form high aspect ratios. With the present parameters ($v_3=0.1$) we found an aspect ratio of 22 to be sufficient to give the lowest ground state with the symmetric formation. The stability of the symmetric formation was also seen in the time-dependent calculations, where the strongly cigar-shaped condensates showed no signs of symmetry breaking (see Fig. 7). In this case the repulsive interaction between the two condensates produces a barrier between the different configurations, resulting in an improved stability.

There is, however, more to this situation. The aspect ratio alone is no guarantee of stable symmetric formations. The interaction strengths v_1 and v_2 , for instance, also play crucial roles. By varying v_1 we showed that the high-aspect-ratio case may go from having a symmetric ground state to a symmetry-broken ground state (see Fig. 5).

In this paper we have tried to give a glimpse of the truly rich and complex behavior of these systems. To cover all parameter regions for the two-component condensate completely is a formidable task, which would require an investigation of the relation between the aspect ratio, the particle numbers, and the three scattering lengths.

ACKNOWLEDGMENTS

The author wishes to thank Stig Stenholm for useful remarks and comments, and Eric Cornell for discussing recent experimental data. The Finnish Center for Scientific Computing (CSC) is acknowledged for providing the computer time.

-
- [1] M. H. Anderson, J. R. Ensher, M. R. Matthews, C. E. Wieman, and E. A. Cornell, *Science* **269**, 198 (1995).
 - [2] K. B. Davis, M.-O. Mewes, M. R. Andrews, N. J. van Druten, D. S. Durfee, D. M. Kurn, and W. Ketterle, *Phys. Rev. Lett.* **75**, 3969 (1995).
 - [3] C. C. Bradley, C. A. Sackett, J. J. Tollett, and R. G. Hulet, *Phys. Rev. Lett.* **75**, 1687 (1995).
 - [4] C. J. Myatt, E. A. Burt, R. W. Ghrist, E. A. Cornell, and C. E. Wieman, *Phys. Rev. Lett.* **78**, 586 (1997).
 - [5] D. S. Hall, M. R. Matthews, J. R. Ensher, C. E. Wieman, and E. A. Cornell, *Phys. Rev. Lett.* **81**, 1539 (1998).
 - [6] P. Öhberg and S. Stenholm, *Phys. Rev. A* **57**, 1272 (1998).
 - [7] Th. Busch, J. I. Cirac, V. M. Perez-Garcia, and P. Zoller, *Phys. Rev. A* **56**, 2978 (1997).
 - [8] B. D. Esry and C. H. Greene, *Phys. Rev. A* **57**, 1265 (1998).
 - [9] H. Pu and N. P. Bigelow, *Phys. Rev. Lett.* **80**, 1130 (1998).
 - [10] H. Pu and N. P. Bigelow, *Phys. Rev. Lett.* **80**, 1134 (1998).
 - [11] D. Gordon and C. M. Savage, *Phys. Rev. A* **58**, 1440 (1998).
 - [12] D. S. Jin, J. R. Ensher, M. R. Matthews, C. E. Wieman, and E. A. Cornell, *Phys. Rev. Lett.* **77**, 420 (1996).
 - [13] D. S. Jin, M. R. Matthews, J. R. Ensher, C. E. Wieman, and E. A. Cornell, *Phys. Rev. Lett.* **78**, 764 (1997).
 - [14] M.-O. Mewes, M. R. Andrews, N. J. van Druten, D. M. Kurn, D. S. Durfee, C. G. Townsend, and W. Ketterle, *Phys. Rev. Lett.* **77**, 988 (1996).
 - [15] D. M. Stamper-Kurn, M. R. Andrews, A. P. Chikkatur, S. Inouye, H.-J. Miesner, J. Stenger, and W. Ketterle, *Phys. Rev. Lett.* **80**, 2027 (1998).
 - [16] F. Dalfovo and S. Stringari, *Phys. Rev. A* **53**, 2477 (1996).
 - [17] B. D. Esry, C. H. Greene, J. P. Burke, and J. L. Bohn, *Phys. Rev. Lett.* **78**, 3594 (1997).
 - [18] M. J. Holland, D. S. Jin, M. L. Chiofalo, and J. Cooper, *Phys. Rev. Lett.* **78**, 3801 (1997).
 - [19] M. Kira, I. Tittonen, and S. Stenholm, *Phys. Rev. B* **52**, 10 972 (1995).
 - [20] M. R. Matthews, D. S. Hall, D. S. Jin, J. R. Ensher, C. E. Wieman, E. A. Cornell, F. Dalfovo, C. Minniti, and S. Stringari, *Phys. Rev. Lett.* **81**, 243 (1998).